Optical Spectra and Conductivities of Thin Films of the Electride K^+(cryptand[2.2.2])e^-

James Erik Hendrickson† and William P. Pratt, Jr.

Department of Physics and Astronomy and Center for Fundamental Materials Research, Michigan State University, East Lansing, Michigan 48824

Richard C. Phillips and James L. Dye*

Department of Chemistry and Center for Fundamental Materials Research, Michigan State University, East Lansing, Michigan 48824

Received: December 18, 1997; In Final Form: March 24, 1998

Optical and electrical measurements on vapor co-deposited thin films of the most conducting electride, K^+(cryptand[2.2.2])e^-, show results similar to those obtained with polycrystalline pellets and with thin films prepared by solvent evaporation. Initial optical absorbance spectra of films deposited below −50 °C showed contributions from several species, but these spectra evolved with time (annealed) at low temperatures to yield mostly plasmalike spectra, characteristic of marginal metals. Most films deposited at −40 °C showed no change in shape with time, indicating that annealing had occurred during deposition. Four-probe conductivity measurements showed activated temperature dependence with an activation energy of about 0.03 eV, while two-probe conductivity measurements showed similar activation energies, but with a variable resistive barrier at the sample−electrode interfaces. The correlation between conductivities and the decay of the absorbance spectra during decomposition was investigated. Thermal decomposition of the electride films leads to complex conductivity behavior. Except when the temperature is increased very slowly, the films become *more* conducting during the first 40−50% of decomposition, and then the films rapidly become insulating. The conductivity may be due to defect holes that can disappear by annealing or slow decomposition or can be produced during the early stages of rapid decomposition. Alternatively, variable grain-boundary resistance could be responsible. The optical and electrical behavior of the films is correlated with the cavity−channel geometry of this electride.

Introduction

Alkalides and electrides are crystalline ionic salts in which complexed alkali metal cations are counterbalanced by alkali metal anions and stoichiometrically trapped electrons, respectively.[1−6] While over 40 alkalides have been synthesized and structurally characterized since the first one was identified 23 years ago,[7] only seven electride crystal structures have been obtained due to difficulties in growing suitable single crystals. While a given alkalide usually exists in only one crystalline phase, whether rapidly precipitated or grown as single crystals, electrides can have different phases depending on the conditions used in synthesis and/or the thermal history of the sample.[8−10] Electron trapping in cavities and interactions through connecting channels make electrides unique examples of "electron lattice gases" whose optical, electronic, and magnetic properties can be correlated with the geometries of their void spaces.[11,12] Because electride behavior is complex and varied and there are no established models for comparison, it is important to measure as many properties of films, powders, and single crystals as possible in order to provide structure−property correlations. This, in turn, should provide impetus for the construction of theoretical models of these unusual materials.

The title compound, K^+(cryptand[2.2.2])e^- [abbreviated as K^+(C222)e^-], is very different from other electrides in structure and properties. Electron spin pairing is pronounced,[13] and the specific conductivity (σ) of powdered samples is as much as 10 orders of magnitude greater than that of other electrides, reaching values as high as 30 ohm^{-1} cm^{-1}.[14]

The unusual feature of the structure of this electride is that the packing of the complexed cations leaves closely spaced *pairs* of cavities in the lattice.[13,15] The "dumbbell-shaped" cavity pairs are similar to those that form the anionic sites of anion pairs in K^+(C222)K^- and Rb^+(C222)Rb^-.[16] These cavities, which serve as the trapping sites for electrons in K^+(C222)e^-, and the interconnecting channels between these cavities, are displayed in the series of isosurfaces shown in Figure 1. These images were produced by using a recently created set of computer programs that use the known structure of a crystalline compound to produce images (isosurfaces) of the *vacant* spaces.[11,17,18] The programs also allow manipulation of representations of the 3D geometries of the cavities and channels. As the distance of the isosurface to the nearest van der Waals surfaces of the atoms is increased (Figure 1A−C), only the broader interconnecting channels remain visible. These are the channels that, according to theory, should play the major role in interelectron coupling and presumably also in conductivity. It is clear from these representations that the cavities and channels in crystalline K^+(C222)e^- form infinite chains of cavity *dimers* with large diameter intercavity channels. These chains are interconnected within a plane by longer, narrower channels to form a 2D network of cavities and channels. A view perpendicular to these planes (Figure 1D) shows that there are no appreciable channels that interconnect these planes.

* To whom correspondence should be addressed.
† Current address: Department of Physics and Astronomy, University of Wisconsin−Eau Claire, Eau Claire, WI 54702.

S1089-5647(98)00564-1 CCC: $15.00
Published on Web 04/28/1998

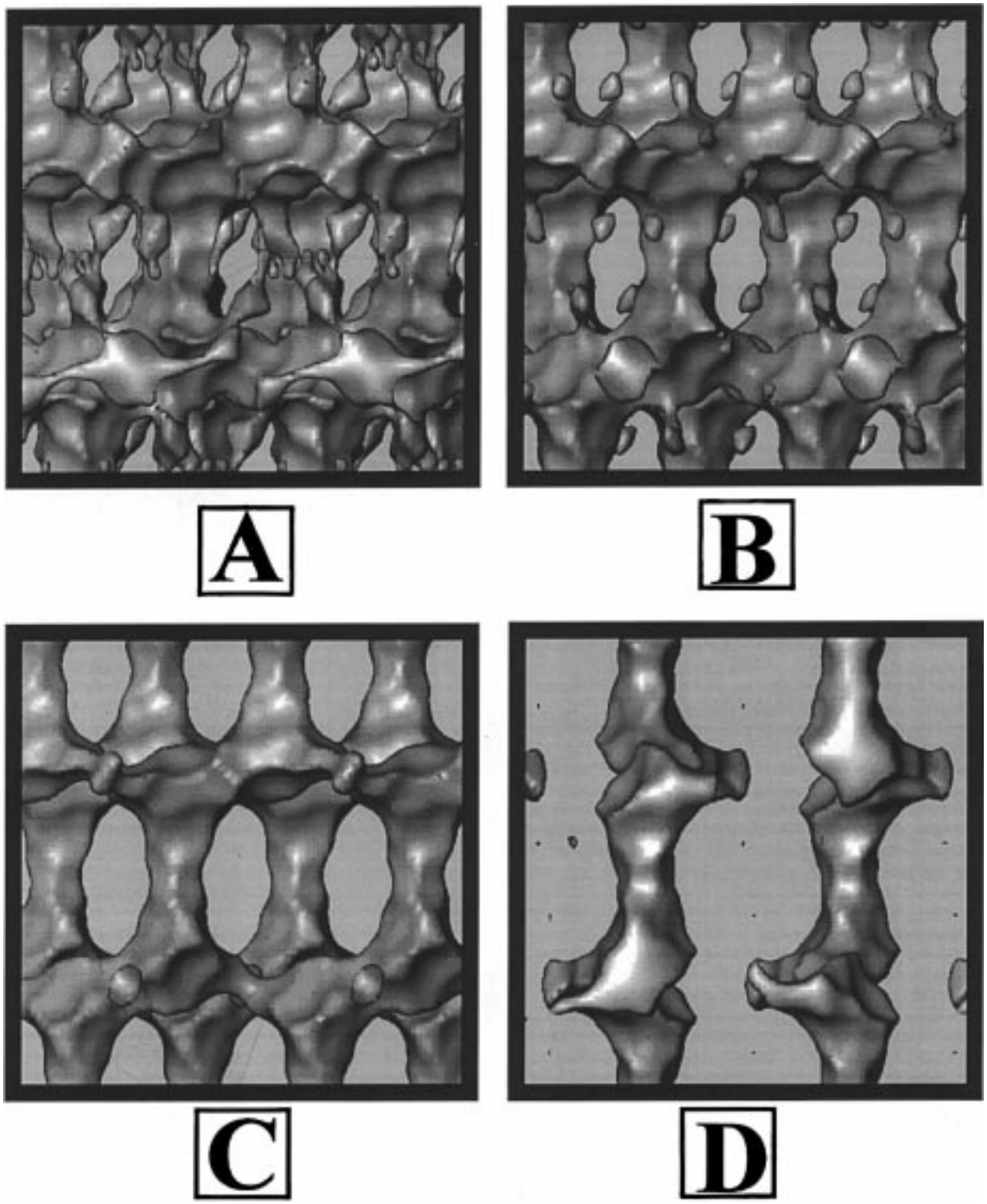

Figure 1. Isosurfaces of the void spaces in the crystal structure of $K^+(C222)e^-$. Views A, B, and C are at 0.46, 0.64, and 0.91 Å from the van der Waals surfaces of the atoms, respectively, and show the major and minor channels that interconnect the dumbbell-shaped cavities. View D is perpendicular to the other views and is an isosurface at 0.82 Å from the atomic surfaces. It shows the absence of significant connecting channels between the 2D arrays of cavities and channels shown in views A−C.

A complication in studying alkalides and electrides is that they decompose readily at higher temperatures (typically > -40 °C) and react rapidly with air and moisture. Thus, all operations with these compounds must be performed under an inert atmosphere or in vacuo and at low temperatures. In addition, defect trapped electrons in alkalides, and alkali metal anions or vacancies in electrides, may affect the physical properties, especially conductivities and activation energies. Adding to these difficulties is the tendency of electrides to form disordered phases as the temperature is increased, even without significant decomposition. Apparently, the complexant molecules can move in such a way that they block channels and decrease the interelectron coupling.[12,19] Thus, care must be used in correlating crystal structures with the results obtained in the study of powders and films.

Previous studies of $K^+(C222)e^-$ included the determination of its crystal structure and measurement of its magnetic susceptibility,[13] powder conductivity,[14] and ^{39}K NMR spec-

trum.[20] The optical spectra of thin films produced by rapid solvent evaporation were also obtained.[21,22]

The magnetic susceptibility as a function of temperature shows that the ground state is a singlet with gradual population of a paramagnetic state or states as the temperature is increased. At the highest temperature permitted by the thermal instability of the sample, 250 K, the molar susceptibility is only 13% of the value expected for free spins. As described in a forthcoming paper, the susceptibility consists of a "Curie tail" (sample dependent) plus an increase with temperature that is consistent with an ALCHA (alternating linear chain Heisenberg antiferromagnetic) model with $-J/k_B > 300$ K and $-J'/J \approx 0.85$. (k_B is the Boltzmann constant, and J and J' are the interelectron coupling constants.) Thus, the magnetic susceptibility is in accord with the structure, in that there is strong pairwise coupling of electron spins in the dumbbell-shaped cavity pairs and only slightly weaker coupling to spins in adjacent cavities. The effect of interchain coupling is not apparent from the susceptibility but may be masked by the Curie tail.

The optical spectra of thin films of many alkalides and electrides have been measured.[21−23] Alkalides show strong ns^2 to $nsnp$ transitions in the visible and near-IR (650−1100 nm). Several electrides, whose crystal structures show the presence of nearly isolated trapped electrons, have well-defined absorbance peaks in the near-infrared (1200−1800 nm). Previous determinations of the optical spectrum of K^+(C222)e^- were confusing, since they showed different spectra depending on the sample's mode of formation and past history. Some of the thin films formed by rapid solvent evaporation had "plasmalike" absorbance spectra that increased throughout the visible region and into the near-infrared region.[22] Other films had a combination of the alkalide (K^-) peak in the visible and a trapped electron peak in the near-infrared.[21] The spectra of some thin films, prepared by controlled co-deposition of K metal and C222 in an apparatus similar to that used in this work, changed with time to plasmalike absorbances.[24] This behavior is indicated by two of the spectra shown in Figure 2. It was not clear whether these synthesis-dependent effects resulted from the rate of solvent removal or from nonuniformity in thickness and/or stoichiometry of the films. A simple borosilicate glass apparatus produced the first vapor co-deposited alkalide and electride films.[25]

Large single crystals of alkalides and electrides are difficult to prepare and are so reactive and thermally unstable that we have not been able to attach conductivity leads, thus preventing single-crystal conductivity studies of these compounds. As a result, all previous dc and ac conductivity studies of alkalides and electrides, except for some two-probe studies of single crystals of Na^+(C222)Na^-, have been made on pressed powders or pellets.

Early temperature-dependent dc conductivity studies of pressed powder samples of many alkalides and electrides demonstrated semiconductor-like behavior with apparent band gaps of 0.6−2.4 eV. Much conductivity-related work has been done specifically on the K^+(C222)e^- system, mostly using polycrystalline samples prepared by precipitation from solvent mixtures. Various measurements indicated that this electride might be metallic: optical absorbance (broad, plasmalike absorbance throughout the visible and near-IR regions), magnetic susceptibility (singlet ground state with nearby [0.03 eV] paramagnetic states), X-ray crystal structure (large, two-dimensional channels connecting paired electrons), and EPR (high microwave conductivity). Measurements of the dc and ac conductivities on pressed powders and pellets of K^+(C222)e^- showed, however, semiconductor-like behavior with apparent activation energies of 0.043 and 0.028 eV above and below −135 °C, respectively. They also showed that there exists either a Schottky barrier or a voltage-dependent resistive barrier at the sample−electrode interface. In addition, the impedance spectroscopy results, particularly the nonzero intercept at high frequencies and the magnitude of the sample capacitance, strongly indicated dominance by grain-boundary effects.[14] The studies described in the present paper used thermally evaporated K metal and C222 to form solvent-free thin polycrystalline films. The grain sizes and grain boundaries may have been different from those of the pressed powder samples, and grain orientation might also have occurred. Crystals tend to form as flat plates that might influence their orientation. In the present work, dc conductivity measurements and optical absorbance spectra were made simultaneously on vapor-deposited thin films of K^+(C222)e^- of known overall composition.

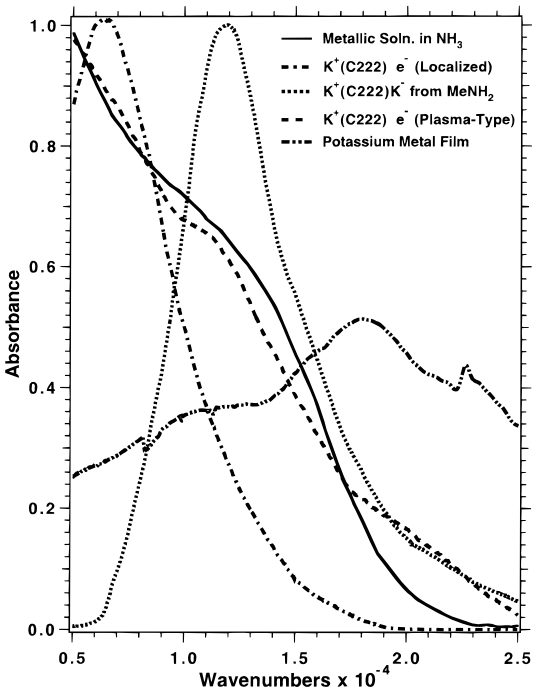

Figure 2. Model normalized spectra obtained in earlier experiments. The spectrum of K^+(C222)K^-, the plasma-type spectrum of K^+(C222)e^-, and the spectrum of potassium metal (not normalized) were used to fit the film spectra observed in this work.

Experimental Section

A modification of the thermal vapor deposition apparatus previously described in detail[26] produced the electride films. The apparatus was modified in two significant ways: the appropriate electronics was added, both within the bell jar and externally, to allow measurement of thin-film conductivities, and a fiber-optic system was incorporated to measure the optical absorbance spectra. The apparatus permitted controlled co-deposition of potassium metal and C222 onto a cooled (−90 to −30 °C) sapphire substrate. Both the overall stoichiometry and the thickness could be controlled to within ∼10%. The conductivity and optical absorbance of the films (typically between 1000 and 2000 Å thick) were then measured in situ. The measurement of thin-film optical spectra has been described in detail elsewhere.[27]

The conductivity was measured by two different methods. The first method used a two-probe dc conductivity arrangement. The two chrome/gold electrode combs (50 Å of chrome and

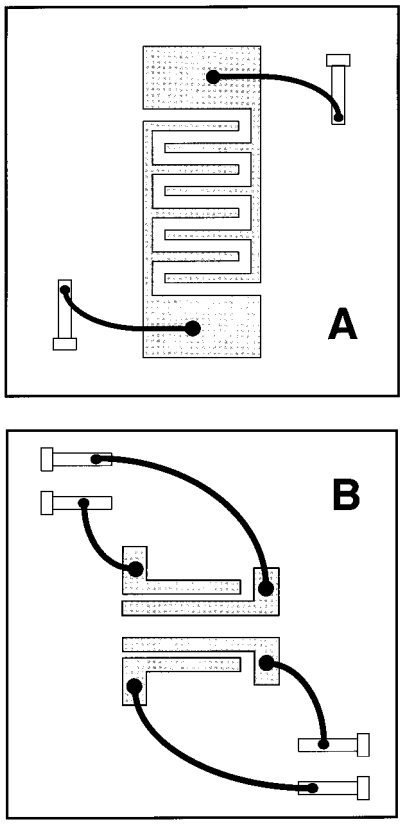

Figure 3. Diagrams of the conductivity geometries used in this work. The shaded regions are the chromium−gold deposits on the sapphire substrate. View A is the two-probe arrangement while view B represents the four-probe geometry.

200 Å of gold) were thermally deposited onto the sapphire substrate prior to use (Figure 3A). The tines of the combs interlace with each other to produce a 0.4 mm gap between the anode and cathode for thin-film conductivity studies. Fine gold wires connected the electrodes to Samtec pin connectors[28] that were epoxied onto the edge of the substrate. Conducting silver epoxy[29] attached the gold wires to the electrodes and pin connectors. A voltage source provided a variable bias voltage, V_B (0−15 V), to the cathode. A simple current-to-voltage feedback amplification circuit inside the apparatus measured the current. The wire from the sample to the amplifier was made as short as possible to avoid picking up and amplifying background noise. The amplification circuit employed an operational amplifier with a 1 MΩ feedback resistor, R_{FB}, to give an amplification factor of 10^6. The amplifier converted the current going through the sample into an output voltage, V_o, which was measured with an *XY* recorder. These data were converted to the resistivity, ρ, by the equation

$$\rho = 1/\sigma = R_S(\text{area})/(\text{length}) = (V_B R_{FB}/V_o)(w_g t_f)/d_g \quad (1)$$

in which R_S is the sample resistance, t_f is the film thickness, w_g is the total length of the anode/cathode gap, and d_g is the distance between the anode and the cathode.

The other method for measuring the conductivity was the four-probe arrangement shown in Figure 3B. Four chrome/gold electrodes were used. A self-balancing 17 Hz conductance bridge supplied a variable known current to the outside electrodes until the measured voltage between the inner electrodes reached a preset value of at most 300 μV. The conductance bridge also allowed two-probe measurements between several combinations of electrodes.

The temperature of the sample was controlled by manual regulation of the flow of cooled gaseous nitrogen through the copper block that holds the substrate. A thermocouple continuously monitored the temperature of the copper block. A hole in the copper block directly below the center of the substrate (where the electride film was located) allowed light to pass through for optical absorbance measurements. The good thermal conductivity of the sapphire substrate kept the temperature of the film within a few degrees of the copper block temperature, even while being illuminated by the white light source. This was verified in control experiments in which a thermocouple was attached to the center of the sapphire substrate.

The gaps between the electrodes allowed the measurement of the optical absorbance of the electride during the experiment. A number of runs were also made by deposition on an electrode-free substrate. A model 260 Guided Wave spectrophotometer measured the optical absorbance of the films. Fiber-optic cables carried the light in to and out of the apparatus through a custom-built vacuum feedthrough. The ends of the fibers were positioned above and below the substrate and included light-collimating lenses. A typical scan from 400 to 1700 nm took less than 60 s. This is a significant improvement over the earlier method employed for measuring optical absorbance.[26] Second-order reflection from the single grating in the monochromator prevented reliable measurement at wavelengths greater than 2000 nm.

A typical run consisted of four steps: loading, evacuation, deposition, and measurement. The potassium metal and purified C222 were stored in a Vacuum Atmospheres helium-filled glovebox. The cleaned sample boats were heated in an oven to ∼110 °C and then brought into the glovebox. Potassium metal (∼0.1 g) and C222 (∼0.2 g) were weighed and placed in their respective boats. Purified octane covered the air-sensitive potassium to protect it during the transfer from a sealed container to the bell jar apparatus. A mechanical roughing pump was used to evacuate the bell jar, after which a CTI cryopump achieved a base pressure of $<10^{-7}$ Torr. Cold nitrogen gas cooled the substrate to the desired deposition temperature and also cooled the film thickness monitors and a "chimney" over the complexant to −80 °C or below (to prevent reevaporation of complexant). Under computer control of the heating power, the temperatures of the thermoelectric cooler for the C222 and of the resistively heated metal boat for the potassium were increased until the deposition rates were at the proper stoichiometry for a one-to-one (or other) ratio of K metal to C222. The substrate was then rotated into the confluence of the vapor streams. It was necessary to constantly monitor the deposition rates of the two vapor streams and to change the boat temperatures in order to maintain the desired stoichiometry. Although such deviations were small during the deposition, they can result in regions of nonstoichiometry even though the overall stoichiometry could be controlled to within about 5%. When the appropriate thickness was obtained, the substrate was rotated to the position of the optical system and the absorbance spectrum was measured. At this point, the conductivity was also monitored in some runs. The optical and/or electrical properties of the film could be measured at temperatures between −100 ° and +10 °C. However, these electride films undergo irreversible thermal decomposition that generally starts at about −30 °C. As described below, the optical spectra also depend somewhat on the substrate temperature during deposition.

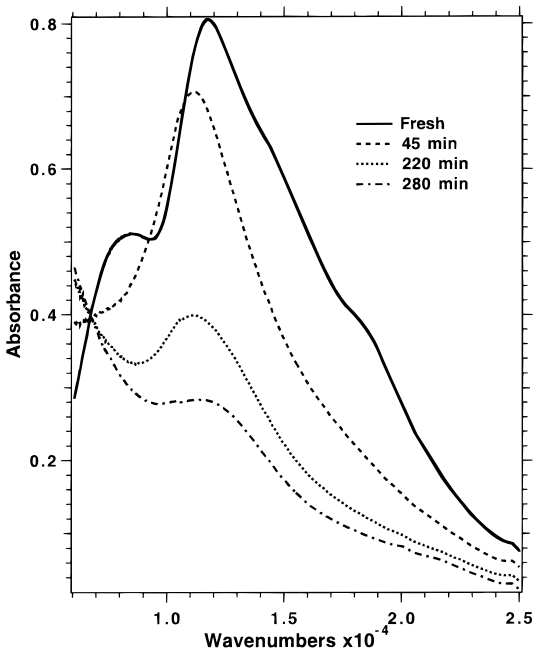

Figure 4. Evolution of the absorbance spectrum of a 1665 Å thick film of K^+(C222)e^- deposited and annealed at −60 °C (run 12/21/93). Note the isosbestic point at 7000 cm^{-1} and the conversion during annealing of the peaks of K^- and of e^- (local) and the shoulder of K (metal) to a nearly plasmalike spectrum.

Results

Optical absorbance spectra of stoichiometric vapor co-deposited K^+(C222)e^- thin films were obtained at wavenumbers from 600 to 25 000 cm^{-1} (wavelengths from 1700 to 400 nm). Figure 4 shows a typical initial absorbance spectrum of a film deposited at −60 °C as well as its change with time at constant temperature. Spectra obtained under these conditions generally have four features: a major absorbance peak at 11 500 cm^{-1}, a smaller peak or shoulder at 7200 cm^{-1}, a minor shoulder at 18 000 cm^{-1}, and a plasmalike absorbance that decreased steadily from low to high wavenumbers. The 11 500 cm^{-1} peak is similar in position and shape to the potasside peak of the alkalide K^+(C222)K^-. The presence of this peak indicates that initial electride films often contain appreciable amounts of potasside. The 7200 cm^{-1} peak probably corresponds to the absorbance of locally trapped electrons that cannot interact strongly enough to form a plasmalike spectrum. The less prominent feature with a broad shoulder at 18 000 cm^{-1} may correspond to the presence of small amounts of potassium metal in the film (see Figure 2). All of the "impurity" features are probably present because of initial inhomogeneities in the film and/or slow migration and cation encapsulation at the lower deposition temperature. The potassium metal shoulder and the trapped electron peak disappeared as the films "annealed" at −60 °C. The K^- absorbance decreased more slowly at −60 °C to become a minor contributor in the annealed film, although small contributions were often present even after the spectra stabilized. Data on film thickness, deposition temperature, and annealing time are given for all films of overall stoichiometry 1:1 in Table 1. The annealing time varied from run to run, from as little as 11 min to as long as 960 min. Of 19 films prepared at −60 °C, three annealed so slowly that substantial decomposition occurred during annealing, and the conversion to the plasmalike spectrum was not complete. One film deposited at this temperature showed little initial K^- absorption, and the spectral shape remained constant similar to the behavior of most films deposited at −45 °C or higher (see below).

The remaining 15 films deposited at −60 °C or below had an isosbestic point at 7000 cm^{-1}. The long-time stability of the annealed spectrum at −60 °C indicated that, during the annealing process, the films were not decomposing appreciably, but rather were undergoing a conversion from an electride plus "impurities" to a more nearly pure electride. For example, the last spectrum of Figure 4 was stable for many hours in the vacuum system at temperatures at or below −60 °C. At higher temperatures, two processes occurred: disappearance of any residual K^- absorbance and decomposition of the entire electride film. As decomposition occurred, the plasmalike absorbance of the electride began to decrease with both increasing temperature and the passage of time, but without any change in shape. When films were deposited with a slight excess of C222, the optical spectra were similar to those of stoichiometric films. The annealing and decomposition characteristics of these C222-rich films were also very similar to those of stoichiometric electride films.

When films of nominal stoichiometry K^+(C222)K^- were deposited at −60 °C, both a substantial K^- peak and a peak at 7000 cm^{-1} were present along with some K metal absorbance. There was little or no plasmalike character. The shape remained constant during the initial stages of decomposition. Only after considerable decomposition had occurred did such films exhibit substantial plasmalike absorbance.

Stoichiometric films of K^+(C222)e^- deposited at ∼−40 °C showed different spectral and temporal behavior than those deposited at or below −60 °C. Usually the spectrum consisted of a single broad peak at 7800 cm^{-1} along with a broad underlying plasmalike absorbance. Typical spectra are shown in Figure 5. When the initial spectrum showed little or no K^- contribution, there was no change during constant temperature annealing, and the spectral shape also remained essentially unchanged during decomposition at higher temperatures. Two of the seven films listed in Table 1 that were prepared at −35 to −45 °C showed an initial K^- peak and annealed to a plasmalike spectrum, similar to the behavior of films deposited at −60 °C and below. There was no change with temperature of the spectral shapes of "annealed" films prepared at either temperature. The two types of behavior were determined at the time of deposition and did not interconvert. Apparently, at the higher temperature, annealing usually occurred during deposition.

The dramatic decrease in absorbance during annealing at −60 °C (Figure 4) followed by long-time stability of the plasmalike spectrum raised a number of questions. Did the "defect" absorbing species (K^-, K metal, locally trapped electrons) decompose or react with residual gases, or did they convert to a stoichiometric electride with a plasmalike spectrum? If the latter explanation is correct, where is the missing oscillator strength? The increase in absorbance in the infrared at energies below that of the isosbestic point shows that *some* conversion must have occurred, but was it quantitative or only partial? To shed light on such questions, we examined the total oscillator strength of the electronic transitions, including extrapolations outside of the wavenumber regions available in the experiment.

The oscillator strength, f, is given by

$$f = 1.44 \times 10^{-19} \int_0^\infty \epsilon(\nu)\, d\nu \qquad (2)$$

when the integral has the units $cm^2\ mmol^{-1}\ s^{-1}$. The extinction coefficient is related to the measured absorbance through $\epsilon(\nu) = A/Cl$ in which C is concentration of the absorbing species in mmol cm^{-3} and l is the path length in cm. For allowed

TABLE 1: Spectral Properties of Stoichiometric Films of $K^+(C222)e^-$ [a]

film ID (date)	thickness (Å)	deposition temp (°C)	anneal time (min)	oscillator strength		deconvolution (%)[b]		
				measured	extrapolated	K^-	e^-(plasma)	K(metal)
10/10/91	1300	−60	240	0.71 (0.34)	0.80 (0.71)	71 (0)	4 (56)	30 (29)
10/14/91	1375	−60	120	0.60 (0.34)	0.70 (0.56)	64 (13)	9 (68)	29 (17)
11/19/92	960	−60	535	1.12 (0.41)		*c*		
03/03/93	1240	−60	960	1.00 (0.39)		*c*		
05/10/93	1190	−60	20	0.56 (0.32)	0.69 (0.74)	54 (0)	5 (94)	30 (5)
06/07/93	1410	−40	*d*	0.36	0.74	0	56	32
07/20/93	1240	−40	130	0.90 (0.53)	1.08 (1.06)	37 (0)	26 (65)	32 (30)
08/03/93	1690	−35	165	0.82 (0.55)	0.96 (0.89)	41 (0)	20 (73)	27 (30)
09/21/93	1300	−60	30	0.79 (0.54)	1.03 (1.04)	51 (4)	7 (71)	27 (17)
09/23/93	1410	−60	40	0.91 (0.58)	1.06 (1.07)	51 (8)	5 (65)	34 (24)
10/01/93	1695	−60	570	1.33 (0.55)		*c*		
10/09/93	1805	−60	45	0.70 (0.46)	0.86 (0.86)	62 (11)	0 (68)	28 (19)
10/12/93	2090	−60	60	0.71 (0.51)	0.89 (1.06)	57 (12)	10 (64)	24 (21)
10/19/93	2260	−60	50	0.56 (0.39)	0.72 (0.81)	57 (2)	11 (71)	25 (25)
10/26/93	1965	−60	745	0.97 (0.48)	1.13 (1.11)	54 (6)	13 (68)	27 (24)
12/17/93	1695	−60	65	0.84 (0.57)	0.92 (1.02)	46 (8)	15 (69)	33 (21)
12/21/93	1665	−60	280	0.87 (0.36)	0.91 (0.89)	56 (8)	5 (78)	28 (7)
12/29/93	1750	−60	75	0.72 (0.48)	0.79 (0.86)	61 (22)	6 (68)	24 (9)
01/28/94	1750	−60	130	0.81 (0.31)	0.97 (0.68)	44 (5)	20 (94)	31 (0)
02/02/94	2270	−60	275	0.60 (0.48)	0.93 (0.81)	11 (4)	33 (44)	15 (12)
02/17/94	2405	−60	690	0.87 (0.40)	0.97 (0.58)	58 (10)	9 (66)	23 (17)
09/16/96	4558	−45	*d*	0.63	0.96	7	42	21
10/15/96	3782	−45	*d*	0.53	0.85	11	41	24
02/05/97	3310	−40	*d*	0.53	0.77	9	45	27
03/27/97	3285	−40	*d*	0.57	0.84	11	48	21
05/21/97	3954	−60	11	0.59 (0.55)	0.80 (0.84)	12 (3)	53 (57)	19 (20)

[a] Values in parentheses refer to the spectra of annealed films. [b] Deconvolution based on measured not extrapolated spectra. [c] Decomposition during annealing too extensive for analysis. [d] No change in shape with time; annealing complete during deposition.

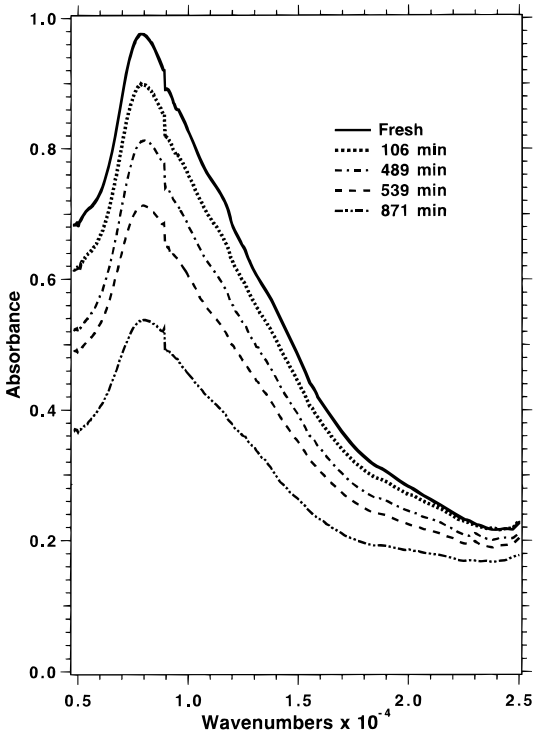

Figure 5. Evolution of the absorbance spectrum of a 3285 Å thick film of $K^+(C222)e^-$ deposited and annealed at −40 °C (run 03/27/97). Note the invariance of the spectral shape. The discontinuity at 9000 cm^{-1} occurs at a grating change and represents drift in this lengthy run.

transitions in a stoichiometric electride film, the *total* oscillator strength should be ≈1.0, whether or not the electron is localized, delocalized, present on K^-, or available as the valence electron of potassium metal. The concentration is known from the density and masses of K and C222. We assume that the density of the film, δ, is the same as that of the crystalline electride. The path length l, is the film thickness in cm. The final expression, including a correction for possible deviations of the metal-to-complexant ratio, R, from its nominal value of 1.0 is

$$f = \frac{4.317 \times 10^{-12}(M_C + RM_M)}{\delta l} \int_0^\infty A(\bar{\nu})\, d\bar{\nu} \qquad (3)$$

in which M_C is the molar mass of the complexant and M_M is that of the metal used.

The proper form of the extrapolation of the absorbance to $\bar{\nu} = 0$ and $\bar{\nu} = \infty$ is unknown. As shown in Figure 6, however, simple linear extrapolations can add appreciable areas outside of the accessible region. In the absence of additional information, we assume that the plasmalike absorbance continues to increase in the infrared in a linear fashion and that straight-line extrapolations to zero absorbance are valid in the high wavenumber region and for the initial spectrum on the low wavenumber side. It should be noted that extrapolation of the plasmalike spectra to zero frequency with a simple Drude expression (see below) gives essentially the same result as linear extrapolation. For the example shown in Figure 6, the areas under the initial spectrum and the annealed (50 min) spectrum, over the measured spectral region, yield oscillator strengths of 0.56 and 0.39, respectively. Inclusion of the extrapolated regions boosts these values to 0.72 and 0.81, respectively. Inspection of Table 1 shows that the total oscillator strengths of fresh films, including the extrapolations, vary from 0.69 to 1.13. In most cases the annealed oscillator strengths are not very different from the initial values. Thus, it is plausible that the apparent "missing" oscillator strength is in the infrared region of the plasmalike absorbance and at wavenumbers higher than are accessible in these experiments. The initial "defect" species may not have decomposed or reacted with residual gases but rather were simply converted to the electride, much of whose absorbance lies outside of the available spectral region. As a

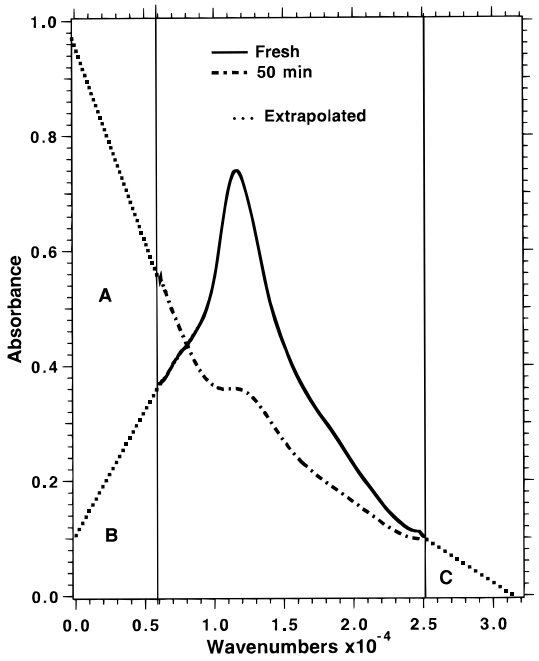

Figure 6. Extrapolation of the spectra obtained for a film of K^+(C222)e^- of thickness 2260 Å deposited and annealed at −60 °C (run 10/19/93). Straight line extrapolations were used.

film decomposes, the oscillator strength decreases and provides a useful measure of the extent of decomposition.

Five of the seven films deposited at −35 ° to −45 °C and included in Table 1 showed little or no initial K^- peak, a peak at 7800−7900 cm^{-1}, and a broad, plasmalike absorption throughout the visible. These films were very stable and exhibited no change in shape during decomposition at higher temperatures. Apparently, whatever annealing may have taken place occurred during the deposition process because of the higher temperature. Oscillator strengths based on extrapolations that included the plasmalike contribution ranged from 0.74 to 0.96.

As indicated above, the spectra probably contain contributions from K^-, "isolated" trapped electrons, potassium metal, and the "plasmalike" electride. To sort out these contributions, the spectra were simulated by using the spectral shapes of K^+(C222)K^-, K^+(C222)e^- (plasmalike), and potassium metal films shown in Figure 2. The first two model spectra were those obtained by rapid evaporation of methylamine from a liquid film on the walls of an optical cell, and that of K metal was obtained in this work by deposition of thin potassium metal films on a partially transparent gold−chromium−sapphire substrate. Deposition of K metal directly on the sapphire substrate resulted in "island" formation with no well-defined spectra below about 500 Å nominal thickness.

A typical deconvolution is shown in Figure 7 for a fresh film and in Figure 8 for an annealed film. Residual spectra, dominated by contributions from localized electrons, are shown for five fresh films in Figure 9. Although the model spectra used may not be completely appropriate for vapor-deposited films, they do permit approximate assignments of the various contributions to the spectra. The percent contributions of the various species for both fresh and annealed films are given in Table 1. Since the spectral shapes of five films deposited at −35 ° to −45 °C generally did not change with time, only the percent contributions of various species to fresh films are given for these runs. It is likely that much of the observed absorbance at higher wavenumbers, not present in the model spectra of K^-

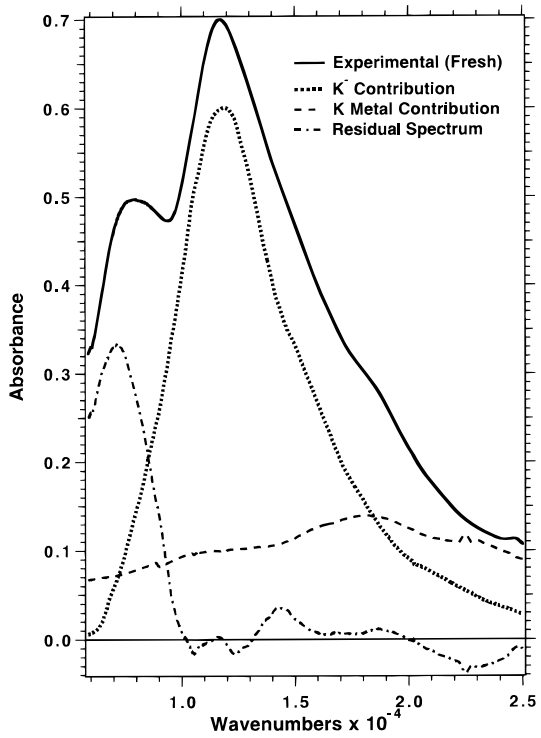

Figure 7. Deconvolution of the spectrum of a fresh film by adjusting the contributions from model spectra. The film was deposited at −60 °C and had a thickness of 1805 Å (run 10/09/93). The residual is dominated by the spectrum of the localized electron.

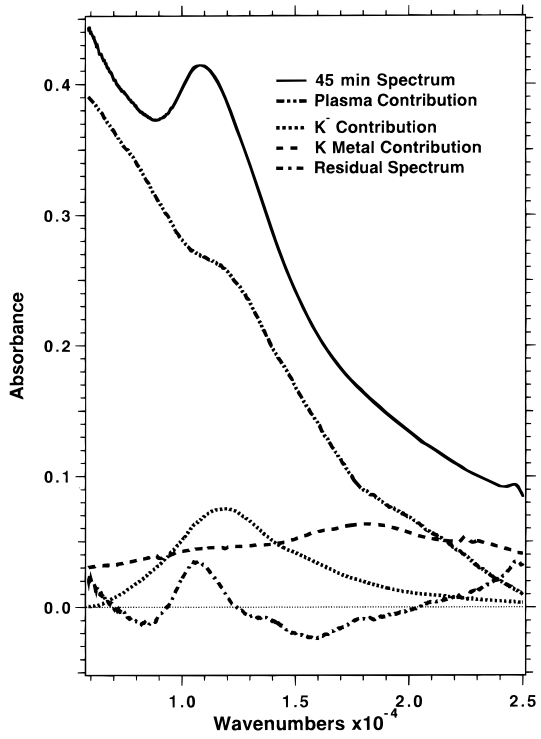

Figure 8. Deconvolution of the spectrum of the film of Figure 7 after annealing at −60 °C. Note the remaining contribution of K^- and the absence of both the peak of e^- (local) and the shoulder of K (metal). The contribution of the latter spectrum probably does not actually result from K metal but was required to account for the remaining absorbance at high wavenumbers not present in the model spectrum of e^- (plasma type).

or e^-_{plasma}, is intrinsic to these films. As a result, the spectral simulation overestimates the amount of K metal actually present in the films, especially for annealed films.

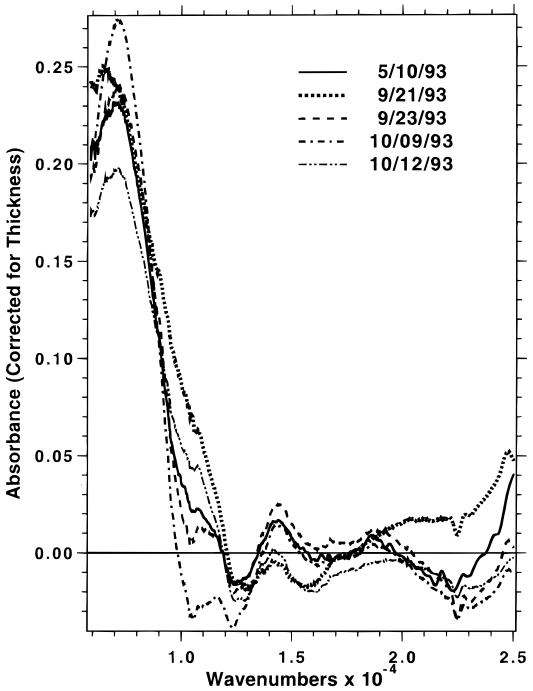

Figure 9. Residual spectra of fresh films obtained by deconvolution with model spectra. The data are from five consecutive −60 °C runs listed in Table 1 and have been converted to a common thickness of 1500 Å. Note that the residual peaks of the localized electron common to fresh films deposited at this temperature have reasonably reproducible shapes and intensities.

The electrical conductivities of 18 films of $K^+(C222)e^-$ were measured, five of them with four-probe methods. The general behavior during temperature changes and decomposition was the same with both methods. However, as with powders and pellets, electrode effects were present that usually yielded lower apparent conductivities and greater run-to-run variability when two-probe methods were used than with four-probe techniques. Table 2 summarizes all of the conductivity data. The apparent initial specific conductivities (σ, in ohm^{-1} cm^{-1}) measured by two-probe methods ranged from 0.059 to 70 with an average value of 7.5, while four-probe methods yielded values ranging from 5.5 to 48 with an average value of 20.8. One two-probe run with three electrodes to yield both wide and narrow spacing resulted in a factor of 2.2 difference in the apparent value of σ, indicating the importance of electrode effects. A four-probe run in which the resistance was measured as a function of film thickness showed that $1/R$ was approximately linear in thickness from 275 to 2400 Å. The value of σ, measured at 20 thicknesses, was 2.6 ± 0.4 ohm^{-1} cm^{-1}. This shows that bulk conductivity rather than surface conductivity is involved. Films made with the stoichiometry $K^+(C222)K^-$ were insulating, with $\sigma < 10^{-5}$ ohm^{-1} cm^{-1}, while a film with a K:C222 ratio of 1.5, identified in Table 2 as run 02/09/94, had an initial value of $\sigma = 0.6$ ohm^{-1} cm^{-1}, which increased to 41 ohm^{-1} cm^{-1} after about 50% decomposition, as measured by the decrease in oscillator strength.

Annealed nondecomposing films showed both two-probe and four-probe conductivities that generally increased slightly with increasing temperature. The variability of the annealing process and the difficulty in separating the effects of annealing from those of decomposition made quantitative studies of the temperature dependence difficult. The apparent activation energies, however, were relatively small, ranging from 0.016 to 0.053 eV, values that are consistent with those obtained from packed powders and pellets (0.028−0.043 eV). The magnitude of σ was also similar with an average of 21 ohm^{-1} cm^{-1} for films at −60 °C compared with ∼15 ohm^{-1} cm^{-1} for packed powders and pellets at this temperature.

TABLE 2: Specific Conductivities of $K^+(C222)e^-$ Films

film ID (date)[a]	specific conductivity (ohm^{-1}cm^{-1}) initial	low[b]	high[c]	act. energy (meV)
05/10/93	0.059	0.033	0.25*	
06/07/93	0.53	0.067	0.67*	16
07/20/93	15	7.7	18.	28
08/03/93	70	5.7	87	
09/23/93	0.41	0.011	0.45	
10/01/93	0.23	0.16	1.0*	29
10/09/93	0.38	0.001	0.45	
10/12/93	0.079	0.064	0.3*	
10/19/93	0.25	0.01	2.0*	
10/26/93	0.90	0.50	6.0*	
12/17/93	0.77	0.30	3.3*	22
12/21/93	5.7	4.0	8.2	32
12/29/93	3.1	1.0	6.4*	38
01/28/94	15	7.8	16	18
02/02/94	29	28	43*	
02/09/94[d]	0.63	0.63	41	24
02/17/94	5.5	5.0	37	
03/27/97	48	7.0	54	
05/21/97	6.7	4.2	6.7	

[a] Two-probe conductivity through 12/29/93 and four-probe after that date. [b] Minimum conductivity before the onset of major decomposition. [c] Asterisk denotes runs during which the highest conductivity occurred at 30−40% decomposition level. [d] Initial ratio of K to C222 was 1.5:1. Peak conductivity occurred at ∼50% decomposition

The time and temperature dependence of the conductivity was most unexpected. We had presumed that the conductivity would increase as the samples "annealed" from a mixture of species to the plasmalike spectra and that decomposition would result in a marked decrease in conductivity. However, the process of "annealing", in which the spectrum of films deposited at −60 °C became plasmalike, usually resulted in only small changes in conductivity, decreasing in seven runs, increasing in five runs, and remaining essentially constant in six runs. Within the run-to-run variability the conductivity was also independent of the temperature of deposition. Thus, the conductivity is remarkably insensitive to the nature of fresh and annealed films as exemplified by their spectra.

Even more surprising was the effect of decomposition on the conductivity. Changes in the oscillator strength provide a measure of the extent of decomposition. To initiate significant decomposition, it was usually necessary to increase the temperature to −30 °C or higher. Remarkably, during the first 30−40% decomposition, the conductivity did not decrease appreciably. In fact, in most cases, rapid decomposition gave an *increase* in conductivity. When the absorbance of the film indicated greater than about 40% decomposition, the conductivity plunged rapidly. Typical four-probe behavior is shown in Figure 10. The results obtained with two-probe conductivity were similar, but as described above, electrode effects were frequently important. As illustrated in Figure 11 for a two-probe run, the conductivity increase upon partial decomposition could be reversed by reducing the temperature. At about 40% decomposition the conductivity decreased dramatically, but as shown in Figure 11, a rapid temperature rise gave a slight increase in conductivity even at 70% decomposition. In a number of experiments, the temperature was increased slowly and maintained at −30 ° to −40 °C. In these cases, the conductivity remained nearly constant during decomposition but once again plunged when the percent decomposition exceeded about 40%.

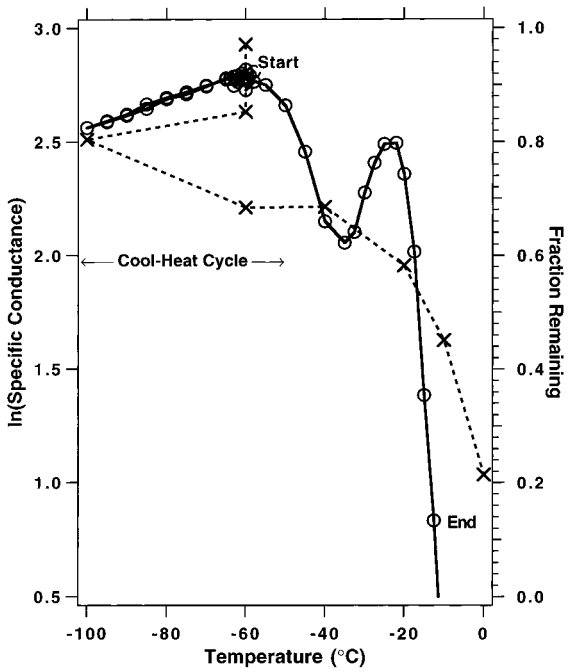

Figure 10. The effect of temperature and decomposition on the four-probe conductivity of a thin film of K^+(C222)e^- (run of 01/28/94). Circles are for conductivity while the points designated by × refer to the fraction remaining, as determined from the measured oscillator strength. The film was deposited at −60 °C and a cool−heat cycle to −100 °C was run after 45 min of annealing in order to estimate the activation energy. After this cycle was completed (at 130 min) the temperature was allowed to increase uniformly at a rate of about 0.4 °C/min until the end of the run at 340 min.

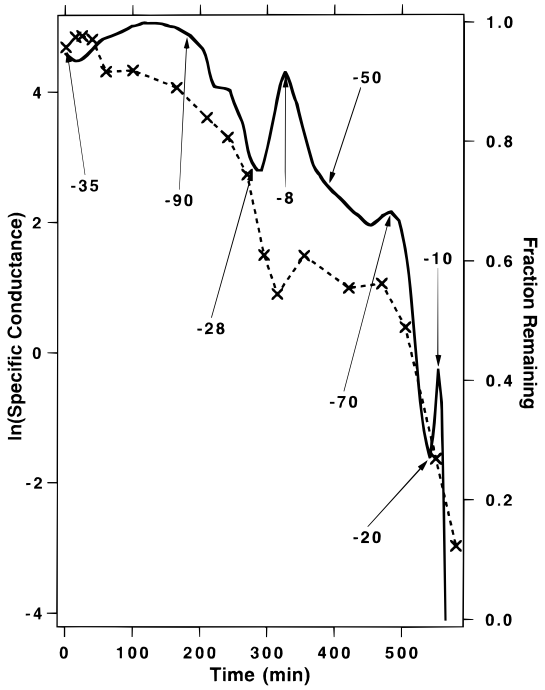

Figure 11. The effect of time, temperature, and decomposition on the two-probe conductivity of a thin film of K^+(C222)e^- (run of 08/03/93). The conductivity is given by the solid line, while the points designated by × refer to the fraction remaining, as determined from the measured oscillator strength. The film was deposited at −35 °C, and the temperature variations during several cycles are indicated on the graph.

Discussion

The optical absorbance spectra of vapor co-deposited films of K^+(C222)e^- are generally similar to those obtained by rapid solvent evaporation. The changes upon annealing, the variable rate of annealing, and the effect of deposition temperature explain why earlier spectra showed such variability in shape. The observed spectra apparently depended on the temperature of deposition, the solvent evaporation rate, the complexant-to-metal ratio, and the time between film formation and determination of the spectra.

The difference between the spectra of films deposited at −60 °C or below and those deposited at −45 °C or above can be explained by differences in the rate of annealing. At the lower temperature, inhomogeneities resulted in the initial formation of substantial amounts of K^- as well as some potassium metal and isolated trapped electrons. Conversion to plasmalike spectra required widely varying amounts of time as K^- was converted into complexed K^+ and two trapped electrons. At the higher temperature, annealing usually occurred during deposition to give a stable spectrum that consisted of a mixture of plasmalike spectra and localized electron spectra.

The similarity between the plasmalike spectra of these films and that of metallic metal−ammonia solutions (∼10 mol % metal) shown in Figure 2 implies a rather high optical conductivity. However, the very broad plasma edge corresponds to a relaxation time of $\sim 10^{-15}$ s and to a short mean-free path of only 4−10 Å according to the classical Drude−Lorentz model of the plasma absorption.[30] The open 1D nature of the cavity−channel chains in this electride is not in accord with the 3D free electron model used in the Drude−Lorentz treatment, but the behavior of randomly oriented crystallites in the film should mimic that of a 3D sample. Regardless of the model used, excited states are available to electrons in K^+(C222)e^- that span the region from <5000 to >25 000 cm^{-1}. In addition, the conservation of oscillator strength during annealing implies a continued increase of the absorbance in the IR at wavenumbers considerably below 5000 cm^{-1} (Figure 6). This suggests that the band gap (if any) between the ground state and excited states is small.

This electride, as is true of all stoichiometric electrides, has a half-filled valence band. Were it not for the presence of rather widely separated trapping sites, one might then expect metallic behavior. However, the Coulomb repulsion that would accompany double occupancy of a cavity and the rather large separation of the cavities, for all other electrides, results in the formation of Mott insulators rather than metals. The case is not so clear with K^+(C222)e^-. The very open cavity−channel structure and the strong pairwise coupling between adjacent electrons in the dumbbell-shaped cavities and to electrons in neighboring cavities indicates substantial overlap of the electron wave functions along the chain. It is possible that this could lead to a plasmalike optical spectrum and near-metallic pseudo-1D conductivity along intact segments of the chain as well as activated interchain electron hopping via the smaller channels shown in Figure 1.

The observation of dc conductivities as high as 30 ohm^{-1} cm^{-1} certainly requires facile charge migration. The key question is the nature of the charge carriers and the resistive barriers that yield a positive activation energy. Previous impedance spectroscopy measurements on packed powders suggest that the intrinsic conductivity is much higher than the bulk dc conductivity; that is, the capacitive component indicates the presence of substantial resistive barriers at grain boundaries.[14] Thus, one possible explanation of the barrier to conductivity is the effect of grain boundaries in powders and films. The unusual variations in conductivity with temperature

and decomposition shown in Figures 10 and 11 could then arise as grain boundary resistance decreased. Since decomposition tends to be autocatalytic, it may occur rapidly within grains, leaving intact conducting paths during the first 30−40% of decomposition. If this explanation is correct, it is surprising that the results are so similar for films and packed powders.

Another possible candidate for the conducting species is missing electrons (holes) produced during film deposition and during decomposition. We anticipate that holes could move rapidly down the cavity−channel chain, as there would then be no Coulomb repulsion between pairs of electrons in the same cavity. When a blocking defect is encountered, the hole could migrate through the interchain channels to an adjacent chain, yielding 2D percolation-type dc conductivity. Decomposition might then have two effects. The first would be blockage of the channel by the decomposition product(s), tending to decrease the conductivity. An offsetting process would tend, however, to introduce more holes. The decomposition process involves the formation of ethylene and leaves behind alkoxide groups in the cryptand,[31] which would surely continue to bind K^+. Each molecule of ethylene formed requires the transfer of two electrons to the residual oxygens to form the alkoxide groups. If the structure of the cryptand is not drastically altered by this process, one or two defect holes might be produced by such decomposition, thus tending to increase the conductivity. As long as a percolation path remains, the observed conductivity might actually increase because of increased hole production, even though the electride is being destroyed by decomposition.

We made a number of attempts to determine the sign of the carriers by means of Hall measurements. Substrates were prepared with the appropriate electrode geometry, and permanent magnets were installed to provide the field. The system was calibrated with films of bismuth and responded appropriately. However, no Hall effect was found with films of $K^+(C222)e^-$. This negative result does not rule out hole conductivity since the Hall coefficients might be small or grain boundaries might interfere with the measurement. Attempts to measure the thermopower of packed powders were also unsuccessful.

It is clear that two kinds of measurements with single crystals would be extremely helpful in understanding the optical and electrical properties of $K^+(C222)e^-$. Reflectance spectra from single crystals over a wide range of wavelengths, together with Kramers−Krönig analysis of the spectra, would provide optical conductivities, dielectric functions, and absorption spectra. Four-probe conductivity studies of single crystals would eliminate grain-boundary effects and would yield intrinsic conductivities. Although it might be possible to measure reflectance spectra as we have done[27] for $Na^+(C222)Na^-$, the surface quality required is difficult to achieve with an electride crystal. It is even more difficult to attach appropriate conductivity leads to these reactive, thermally sensitive crystals, keeping in mind that the temperature would have to be maintained at −60 °C or below. Despite these difficulties, we plan to continue to try to make appropriate single-crystal measurements.

Acknowledgment. This research was supported in part by NSF Grants DMR-94-02016 and DMR-96-10335 and by the Michigan State University Center for Fundamental Materials Research. We are grateful to Deborah Gilbert, Qingshan Xie, and Andrew Ichimura for helpful discussions and for assistance with some of the experiments. We acknowledge useful discussions with Prof. Mark Dykman of the MSU Physics-Astronomy Department about plasma-type absorption spectra.

References and Notes

(1) Dye, J. L. *Prog. Inorg. Chem.* **1984**, *32*, 327−441.
(2) Dye, J. L.; DeBacker, M. G. *Annu. Rev. Phys. Chem.* **1987**, *38*, 271−301.
(3) Dye, J. L. *Science* **1990**, *247*, 663−668.
(4) Dye, J. L. *Chemtracts: Inorg. Chem.* **1993**, *5*, 243−270.
(5) Wagner, M. J.; Dye, J. L. *Annu. Rev. Mater. Sci.* **1993**, *23*, 223−253.
(6) Wagner, M. J.; Dye, J. L. In *Molecular Recognition: Receptors for Cationic Guests*, 1st ed.; Gokel, G. W., Ed.; Pergamon Press: Oxford, UK, 1996; Vol. 1, pp 477−510.
(7) Tehan, F. J.; Barnett, B. L.; Dye, J. L. *J. Am. Chem. Soc.* **1974**, *96*, 7203−7208.
(8) Dawes, S. B.; Eglin, J. L.; Moeggenborg, K. J.; Kim, J.; Dye, J. L. *J. Am. Chem. Soc.* **1991**, *113*, 1605−1609.
(9) Wagner, M. J.; Huang, R. H.; Dye, J. L. *J. Phys. Chem.* **1993**, *97*, 3982−3984.
(10) Huang, R. H.; Wagner, M. J.; Gilbert, D. J.; Reidy-Cedergren, K. A.; Ward, D. L.; Faber, M. K.; Dye, J. L. *J. Am. Chem. Soc.* **1997**, *119*, 3765−3772.
(11) Dye, J. L.; Wagner, M. J.; Overney, G.; Huang, R. H.; Nagy, T. F.; Tomanek, D. *J. Am. Chem. Soc.* **1996**, *118*, 7329−7336.
(12) Dye, J. L. *Inorg. Chem.* **1997**, *36*, 3816−3826.
(13) Huang, R. H.; Faber, M. K.; Moeggenborg, K. J.; Ward, D. L.; Dye, J. L. *Nature* **1988**, *331*, 599−601.
(14) Moeggenborg, K. J.; Papaioannou, J.; Dye, J. L. *Chem. Mater.* **1991**, *3*, 514−520.
(15) Ward, D. L.; Huang, R. H.; Dye, J. L. *Acta Crystallogr.* **1988**, *C44*, 1374−1376.
(16) Huang, R. H.; Ward, D. L.; Dye, J. L. *J. Am. Chem. Soc.* **1989**, *111*, 5707−5708.
(17) Wagner, M. J.; Dye, J. L. *J. Solid State Chem.* **1995**, *117*, 309−317.
(18) Nagy, T. F.; Mahanti, S. D.; Dye, J. L. *Zeolites* **1997**, *19*, 57−64.
(19) Dye, J. L. *Nature* **1993**, *365*, 10−11.
(20) Kim, J.; Eglin, J. L.; Ellaboudy, A. S.; McMills, L. E. H.; Huang, S.; Dye, J. L. *J. Phys. Chem.* **1996**, *100*, 2885−2891.
(21) Dye, J. L.; Yemen, M. R.; DaGue, M. G.; Lehn, J.-M. *J. Chem. Phys.* **1978**, *68*, 1665−1670.
(22) DaGue, M. G.; Landers, J. S.; Lewis, H. L.; Dye, J. L. *Chem. Phys. Lett.* **1979**, *66*, 169−172.
(23) Dye, J. L.; DaGue, M. G.; Yemen, M. R.; Landers, J. S.; Lewis, H. L. *J. Phys. Chem.* **1980**, *84*, 1096−1103.
(24) Faber, M. K. Ph.D. Dissertation, Michigan State University, East Lansing, MI, 1985.
(25) Le, L. D.; Issa, D.; VanEck, B.; Dye, J. L. *J. Phys. Chem.* **1982**, *86*, 7−10.
(26) Skowyra, J. B.; Dye, J. L.; Pratt, W. P., Jr. *Rev. Sci. Instrum.* **1989**, *60*, 2666−2672.
(27) Hendrickson, J. E.; Kuo, C. T.; Xie, Q.; Pratt, W. P., Jr.; Dye, J. L. *J. Phys. Chem.* **1996**, *100*, 3395−3401.
(28) Samtec Inc., 810 Progress Blvd., New Albany, IN 47150.
(29) BIPAX, Tra-Con Inc., 55 North Street, Bedford, MA 02155.
(30) Hendrickson, J. E. Ph.D. Dissertation, Michigan State University, East Lansing, MI, 1984.
(31) Cauliez, P. M.; Jackson, J. E.; Dye, J. L. *Tetrahedron Lett.* **1991**, *32*, 5039−5042.